JCTC Journal of Chemical Theory and Computation

Molecular Modeling the Reaction Mechanism of Serine-Carboxyl Peptidases

Ksenia Bravaya,[†] Anastasia Bochenkova,[†] Bella Grigorenko,[†] Igor Topol,[‡] Stanley Burt,[‡] and Alexander Nemukhin*[,†,§]

Department of Chemistry, M. V. Lomonosov Moscow State University, Moscow 119992, Russian Federation, Advanced Biomedical Computing Center, National Cancer Institute at Frederick, Frederick, Maryland 21702, and Institute of Biochemical Physics, Russian Academy of Sciences, Moscow 119997, Russian Federation

Received February 17, 2006

Abstract: We performed molecular modeling on the mechanism of serine-carboxyl peptidases, a novel class of enzymes active at acidic pH and distinguished by the conserved triad of amino acid residues Ser-Glu-Asp. Catalytic cleavage of a hexapeptide fragment of the oxidized B-chain of insulin by the *Pseudomonas* sedolisin, a member of the serine-carboxyl peptidases family, was simulated. Following motifs of the crystal structure of the sedolisin-inhibitor complex (PDB accession code 1NLU) we designed the model enzyme−substrate (ES) complex and performed quantum mechanical−molecular mechanical calculations of the energy profile along a reaction route up to the acylenzyme (EA) complex through the tetrahedral intermediate (TI). The energies and forces were computed by using the PBE0 exchange-correlation functional and the basis set 6-31+G** in the quantum part and the AMBER force field parameters in the molecular mechanical part. Analysis of the ES, TI, and AE structures as well as of the corresponding transition states allows us to scrutinize the chemical transformations catalyzed by sedolisin. According to the results of simulations, the reaction mechanism of serine-carboxyl peptidases should be viewed as a special case of carboxyl (aspartic) proteases, with the nucleophilic water molecule being replaced by the Ser residue. The catalytic triad Ser-Glu-Asp in sedolisin functions differently compared to the well-known triad Ser-His-Asp of serine proteases, despite the structural similarity of sedolisin and the serine proteases member, subtilisin.

Introduction

Serine-carboxyl peptidases or sedolisins[1−9] are presently assigned to the family S53 of clan SB of serine proteinases (the MEROPS database, URL http://merops.sanger.ac.uk). Following the results of intense recent studies of sedolisins primarily by the methods of X-ray spectroscopy, it has been established that there is overall similarity of two protease families, sedolisins and serine protease type subtilisins: practically all secondary structure elements found in the smaller subtilisins also are present in sedolisins. Although both subtilisins and sedolisins utilize the serine residue as the principal nucleophile, other members of the catalytic triad are different. The second member of the triad Ser-His-Asp in subtilisin, histidine, is substituted in sedolisin (with the triad Ser-Glu-Asp) by a topologically equivalent glutamic acid, while the third residue of the triad, aspartic acid in both enzymes, is contributed by topologically different parts of the structure.

A fundamental question for serine-carboxyl peptidases is whether these enzymes with the triad Ser-Glu-Asp use the catalytic mechanism similar to that of serine proteases[10] with

* Corresponding author e-mail: anem@lcc.chem.msu.ru.
[†] M. V. Lomonosov Moscow State University.
[‡] National Cancer Institute at Frederick.
[§] Russian Academy of Sciences.

10.1021/ct6000686 CCC: $33.50
Published on Web 06/24/2006

Chart 1. Chemical Formula of Pseudoiodotyrostatin Used To Generate a Complex 1NLU with Sedolisin[9]

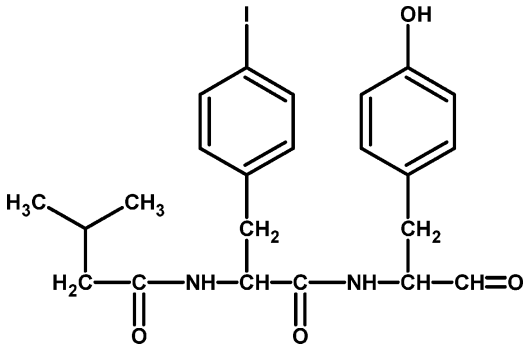

the triad Ser-His-Asp. A practical reason for interest in these enzymes is explained by their potential use in medicine due to activity of the family's member kumamolisin-As as a collagene-degradating agent[6,9] and in industry because of maximum activity at the comparatively low pH of 3−5 and stability of some of these enzymes at high temperatures up to 60 °C.

At present the natural substrates for serine-carboxyl peptidases are unknown, and the knowledge about their structure and function are learned from the experimental studies of the enzymes interacting with different inhibitors. All model inhibitors used in the X-ray studies were peptides with the terminal aldehyde group. In many of these complexes an inhibitor was covalently bound to the enzyme by the hemiacetal bond with the OH group of serine. A 1.3 Å resolution of the structure of the *Pseudomonas* sp. 101 sedolisin (PDB accession code 1NLU),[7,8] in which sedolisin was complexed with two molecules of the inhibitor, pseudoiodotyrostatin (Chart 1), was an important contribution to the field. It was concluded that this structure, in which only one molecule of the inhibitor was covalently bound to Ser, could be viewed as representing the product of enzymatic cleavage of a hexapeptide substrate: the hemiacetal involving Ser287 would represent the complex (or a tetrahedral adduct) formed following nucleophilic attack of the Ser oxygen, while another molecule of pseudoiodotyrostatin would represent the amino product from cleavage.[9]

In this paper we describe the first theoretical simulations of the reaction energy profile and the analysis of the reaction intermediates for the serine-carboxyl peptidases taking the catalytic cleavage of peptide bonds by sedolisin as an important example. Prompted by the crystal structure 1NLU,[8] we designed the model enzyme−substrate (ES) complex and performed calculations of the energy along a reaction route up to the acylenzyme (EA) complex through the tetrahedral intermediate (TI). The model structure corresponding to TI may be directly compared to the experimental moiety 1NLU assigned to "the product complex following enzymatic cleavage of a hexapeptide substrate" or a mimic of the tetrahedral adduct.[7] Therefore, in simulations we constructed the entire reaction profile inspired by the single hint from the experimental studies.

Late in the course of our work, the paper of Guo et al.[11] was published in which the results of quantum mechanical/molecular mechanical and molecular dynamics simulations for the properties of possible tetrahedral adduct in serine-carboxyl peptidases were described. The authors considered the X-ray structure of kumamolisin-As with the inhibitor *N*-acetyl-isoleucyl-prolyl-phenylanial covalently bound to the Ser residue (PDB accession code 1SIO) as a mimic of such adduct. Following the estimates of positions of protons at the nearby residues, Guo et al. concluded that the mode of stabilization of a hypothetical tetrahedral intermediate in serine-carboxyl peptidases may be different compared to that of serine proteases.[11] However, a very limited segment of a possible reaction coordinate was explored in those calculations to confirm the hypothesis on the reaction mechanism.

At preliminary steps of the modeling procedure we applied conventional molecular docking and molecular dynamics simulations, first of all, to determine a reasonable starting position of a model substrate trapped by the enzyme. After that, the reaction energy profile was constructed by using the combined quantum mechanical-molecular mechanical (QM/MM) method,[12−19] which is becoming an important modern tool in studies of enzymatic mechanisms.[20−33] Comprehensive analysis of chemical transformations for the serine protease prototype reactions by the results of previous QM/MM calculations[29−33] provides a suitable basis for comparison.

Theoretical Approaches

Molecular docking calculations were carried out with the Autodock 3.0 program.[34] Molecular dynamics trajectories were computed with the parallel version of the NAMD 2.5 program suite.[35] The most demanding calculations at the combined quantum mechanical−molecular mechanical (QM/MM) level were performed by using the Intel-specific version of the GAMESS(US) program system,[36] PC GAMESS (Granovsky, A. A. URL http://lcc.chem.msu.ru/gran/gamess), specially adjusted for QM/MM calculations. In this program, the mechanical embedding QM/MM technique by Bakowies and Thiel[16] as implemented by Kress and Granovsky was used. The conventional link hydrogen atom approach was applied to interface the QM and MM regions. The energy diagram for the reaction path from the enzyme−substrate complex (ES) to the acylenzyme complex (EA) through the tetrahedral intermediate (TI) was calculated in series of unconstrained and constrained energy minimizations in the QM/MM approximation. Electron polarization of the QM electron density by the protein environment was taken into account by the electronic embedding based QM/MM[16] energy calculations at all stationary points.

As mentioned above, the structures that directly mimic enzyme−substrate complexes are not available from the X-ray studies of sedolisin with appropriate inhibitors. Therefore, selection of a model substrate and construction of the starting configuration of reagents was one of the most difficult tasks of our simulations. By assuming that a model substrate should resemble the covalently bound inhibitor molecule in the 1NLU complex, we choose the hexapeptide fragment corresponding to the residues 22−27 from the insulin oxidized B-chain (PDB accession code 1AIO) known to be hydrolyzed by sedolisin. According to the MEROPS database (URL http://merops.sanger.ac.uk) the cleavage of

Chart 2. Chemical Formula of the Model Hexapeptide Substrate for Sedolisin: Arg-Gly-Phe-Phe-Tyr-Thr

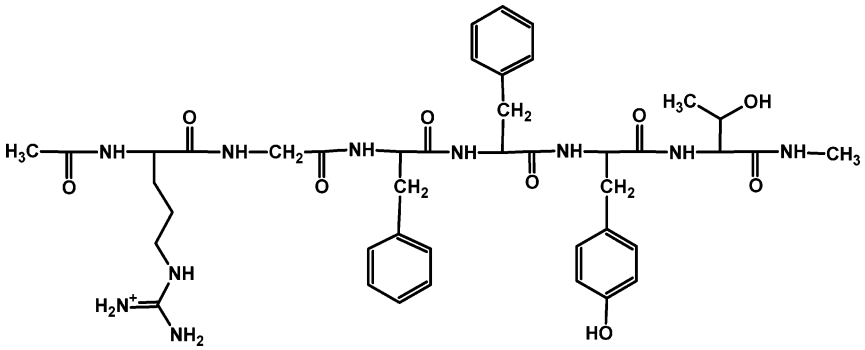

Arg-Gly-Phe-Phe+Tyr-Thr takes place between the Phe and Tyr residues. Therefore, the Phe-Phe fragment of a model substrate (Chart 2) may mimic the Tyr-iodo-Phe moiety (Chart 1) of the covalently bound inhibitor in S1−S2 substrate binding pockets in 1NLU. The concluding residues of the hexapeptide, Arg and Thr, were terminated by the CH_3 groups.

A starting configuration of the ES complex for calculations of the energy profile was created by using molecular docking, molecular dynamics, and the QM/MM approaches. To this goal we deleted the inhibitor molecules from the 1NLU structure and replaced it by the model hexapeptide Arg-Gly-Phe-Phe-Tyr-Thr.

The Lamarckian genetic algorithm was applied for the flexible docking procedure with the AutoDock program package.[34,37,38] The grid maps of the dimension 80 × 80 × 80 were centered on the sedolisin active site. The grid spacing was 0.375 Å, allowing the ligand to explore configuration space within approximately 30 Å from the substrate-binding site. The parameters recommended for the blind docking of flexible ligands by Heteny and Spoel[39] were used. The initial population size used for genetic algorithm was 250, the number of energy evaluation was 10^7, and the maximum number of generations was 1×10^6. The default values of other parameters[34] were used in 100 docking searches. To facilitate the search of suitable positions of substrate, the side chain of Trp136 in the 1NLU structure was slightly shifted from its position in the crystal.

The molecular dynamics simulations (MD) for the enzyme−substrate complex were carried out with the CHARMM force field parameters within the NAMD 2.5 computer package.[35] The protein−substrate complex was buried inside a large cluster of water molecules. The MD trajectories of 80 ps length with a time step of 1 fs initiated from different starting geometry configurations were recorded at 300 K. The protein atoms lying farther than 5 Å from the active site residues were frozen during equilibration. Fifteen of the lowest energy structures obtained in the molecular docking procedure were used as starting geometry configurations. The structures mainly differed in the position of the Tyr26 and Thr27 side chains which occupied two different binding pockets. MD simulation starting from these configurations resulted in two principally different ES geometries, and the one with the lowest energy was used as a starting point for the following computations.

The resulting structure was analyzed in order to locate possible cavities inside the protein near the reaction center to be filled by the water molecules. The surface area of the enzyme which included the substrate binding site was also extensively solvated. The molecular system was thermally equilibrated at 300 K and gradually relaxed to 0 K. The atomic coordinates at the end of trajectories were considered as initial guesses for the subsequent QM/MM geometry optimization for the enzyme−substrate complex.

For QM/MM computations we selected ∼2500 atoms comprising complete coverage of the active site approximately within 10 Å from the atoms of the catalytic residues. Forty-eight atoms of the active site were assigned to the QM-part as illustrated in Figure 1. The energies and forces were

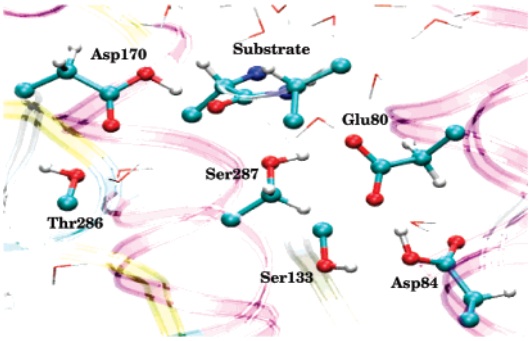

Figure 1. The ball-and-stick representation of the groups included to the QM part of the reacting system.

computed by using the PBE0 exchange-correlation functional and the basis set 6-31+G** in the quantum part and the AMBER force field parameters in the molecular mechanical part.

Partial Hessian analysis was performed at all stationary points located on the potential energy surface. According to this procedure the evaluation of the whole QM/MM force constant matrix was carried out followed by diagonalization of its smaller part corresponding to the QM subsystem.

Results

The structure of enzyme−substrate complex obtained as a minimum energy configuration in the unconstrained QM/MM optimization of geometry parameters is shown in Figure 2.

We note the positions of protons along hydrogen bonds for the most important pairs: (i) Glu80 and Asp84 share a proton which resides on Asp at a very short distance (1.4

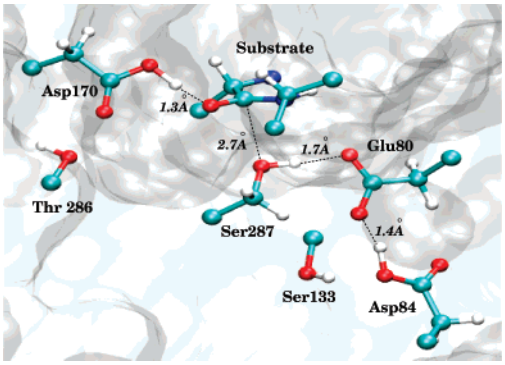

Figure 2. Geometry configuration of the enzyme−substrate complex.

Å) to Glu; (ii) the proton of Ser287 is in perfect position for the move to Glu80; and (iii) the proton of Asp170 is very close (1.3 Å) to the carbonyl oxygen of substrate. We also note a reasonable distance (2.7 Å) from oxygen of Ser287 to carbon of substrate which causes us to consider further developments along the lines typical for serine proteases. Thus, a gradual decrease of this coordinate, the O(Ser)−C(Sub) distance, should lead to the tetrahedral intermediate (TI).[33]

Therefore, we selected the distance (R_{OC}) between the oxygen of Ser287 and the carbon of the substrate as a reaction coordinate for the first stage of the reaction. In a series of constrained minimizations (by keeping fixed values of R_{OC} and optimizing other internal coordinates) we succeeded in locating the equilibrium geometry configuration of the saddle point, or the first transition state TS1, with $R_{OC} = 1.7$ Å. The search of the stationary point corresponding to the tetrahedral intermediate was accomplished as an unconstrained minimization starting from some shorter than 1.7 Å values of R_{OC}. Remarkably, the computed minimum energy path specifies the first proton transfer from Asp170 to the carbonyl oxygen of the substrate occurring at the early values of reaction coordinate. The normal mode of the single imaginary frequency of the first saddle point corresponds to the concerted Asp170 proton transfer and C−O bond formation. Unlike the case of serine proteases, the principal nucleophile, Ser287, donates the proton to its partner in the catalytic triad Glu80 only near the TI configuration. This means that Asp170 plays a crucial role in the reaction mechanism of sedolisin catalysis as an acid activator for the carbonyl group of the substrate. Protonation of the carbonyl oxygen makes this carbonyl group more electrophilic for a subsequent nucleophilic attack by Ser287. In serine proteases, the proton transfer within the catalytic triad from Ser to His aims to activate a nucleophile (Ser) and initialize the chain of transformations, while the role of the oxyanion hole residue(s), analogous to Asp170 in sedolisin, is basically to compensate the developing negative charge on carbonyl oxygen.

The computed structure of the tetrahedral intermediate with the R_{OC} value of 1.5 Å is shown in Figure 3. We note that the third member of the catalytic triad, Asp84, remains protonated at this stage of the reaction.

The energy profile for the route from TI to acylenzyme (EA) was computed by another choice of a reaction

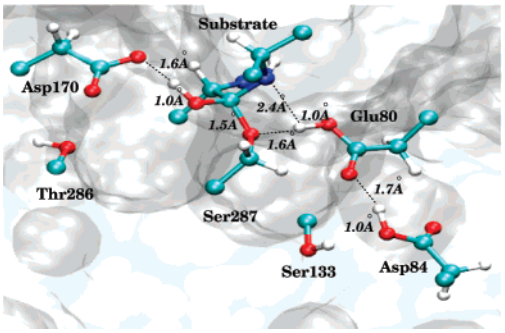

Figure 3. Geometry configuration of the tetrahedral intermediate.

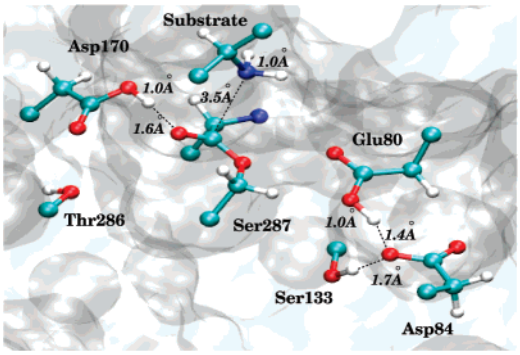

Figure 4. Geometry configuration of the acylenzyme complex.

coordinate. At this stage, the proton initially donated by Ser287 to Glu80 should be transferred to nitrogen of the scissile peptide bond of the substrate. We performed a series of constrained minimizations by gradually decreasing the corresponding H−N distance and locating the second transition state TS2. The normal mode of the single imaginary frequency of the second saddle point corresponds solely to this proton-transfer event. The downhill move toward the acylenzyme complex was carried out as an unconstrained minimization of all internal coordinates. The computed structure of AE is shown in Figure 4.

We note that the scissile peptide bond is cleaved at this point: the distance between initially covalently bound C and N atoms in the hexapeptide is now 3.5 Å. The Asp170 residue restores its protonation status (compare Figures 2 and 3). The Glu80 residue abstracts the proton from the third member of the catalytic triad, Asp84, after losing the primarily transferred proton for the half-product of the hydrolysis reaction.

The computed energy profile for the route from the enzyme−substrate complex (ES) to the acylenzyme complex (EA) through the tetrahedral intermediate (TI) for the peptide bond cleavage of the model hexapeptide Arg-Gly-Phe-Phe+Tyr-Thr by sedolisin is shown in Figure 5. According to these calculations, the activation energy barriers for the reaction are fairly low. The electronic embedding QM/MM results do not alter the mechanistic conclusions qualitatively but reveal additional stabilization of TI by the protein environment. The relative energy of TI is reduced to 5.5 kcal/mol, while the energy barriers are only slightly lowered by 2.8 and 0.8 kcal/mol for TS1 and TS2 saddle points, respectively.

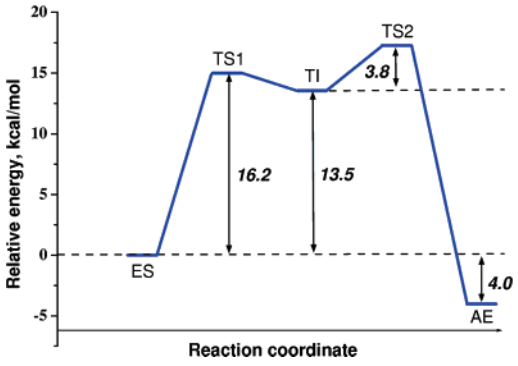

Figure 5. The computed energy diagram for the reaction path from the enzyme−substrate complex (ES) to the acylenzyme complex (EA) through the tetrahedral intermediate (TI) for the peptide bond cleavage of the hexapeptide Arg-Gly-Phe-Phe+Tyr-Thr by sedolisin.

Discussion and Conclusions

As mentioned in the Introduction, the experimentally resolved structure 1NLU refers to the complex of sedolisin with two inhibitor pseudoiodotyrostatin molecules, one of which is covalently bound to Ser287 mimicking a tetrahedral adduct. We can directly compare atomic coordinates of this experimental structure with those obtained in our simulations for the tetrahedral intermediate (TI). The left panel of Figure 6 shows a superposition of experimental and theoretical structures, where blue sticks designate the chains from the crystal moiety 1NLU, and red sticks refer to the calculation results. In the latter case we show the Phe (P1)−Phe (P2)−Gly (P3) fraction of the model substrate. Apparently, two structures are in good agreement, what can be quantitatively characterized by the RMSD values of 0.5 Å calculated for all heavy atoms of the residues in the active site Glu80, Asp84, Ser133, Asp170, Thr286, and Ser287. Even a superposition of substrate P1 and P2 chains on the inhibitor chains shows a remarkable similarity: RMSD is 0.5 Å for P1, and 1.6 Å for P2, and the groups of the model substrate occupy the same binding pockets as the groups of pseudoiodotyrostatin. Therefore, we can conclude that the results of simulations are consistent with the available experimental information.

The reaction mechanism of sedolisin which comes into view in the present work is summarized in Scheme 1. The substrate−enzyme complex (ES), acylenzyme (AE), tetrahedral intermediate (TI), and both transition states (TS1 and TS2) are shown. Step I is the nucleophilic attack of serine oxygen on a carbon atom of the substrate with an enhanced electrophilic character. Structure of the first transition state (Figure 7) clearly demonstrates an acid-based activation

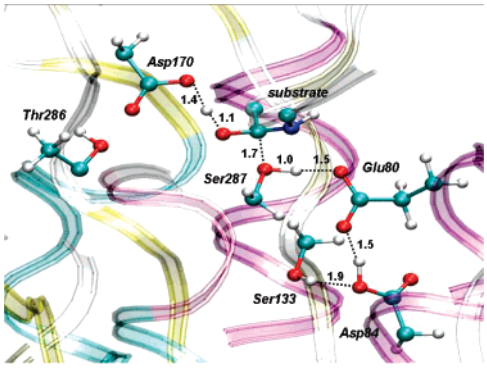

Figure 7. The computed structure of TS1. The distances are shown in Å.

mechanism of the enzyme. The normal-mode analysis at the TS1 configuration also supports the primary role of Asp170 residue, revealing the reaction coordinate being the concerted Asp170 proton transfer and C−O bond formation. Apparently, Glu80 does not play the role of His in the catalytic triad, if the mechanisms of serine-carboxyl peptidases and serine proteases are compared.

In step II, the negatively charged Glu80 acts as a general base to remove the proton from Ser287. A tetrahedral intermediate formed at this stage represents a hemiacetal bonded complex of substrate and the enzyme. Step III includes the activation of the leaving group by the protonated Glu80 which acts as the general acid donating the proton to nitrogen. This step also involves the reorientation of the hydrogen bond of Glu80 from Ser287 to nitrogen of the scissile peptide bond. A structure of the second transition state represents the initial stage of the proton transfer along

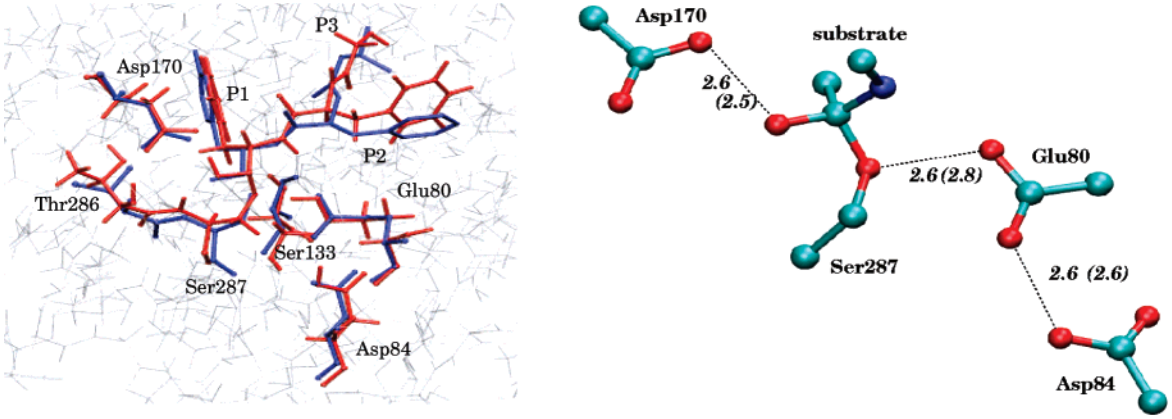

Figure 6. Comparison of the computed structure of TI and the experimental structure 1NLU. Left: superposition of the chains in the active site showing experimental data in blue and computational results in red. Right: equilibrium geometry configuration showing distances in Å; the values in parentheses refer to the calculation results.

Scheme 1. Mechanism of the Catalytic Action of Sedolisin Proposed by the Results of Simulations

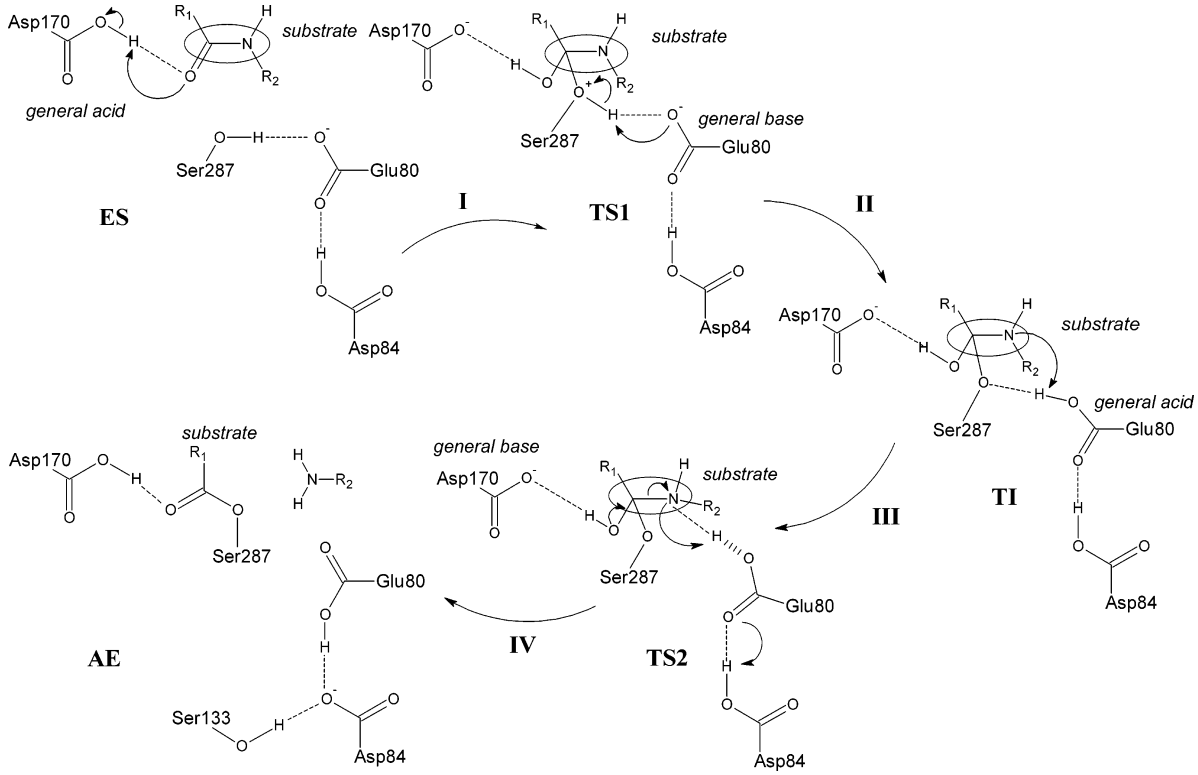

the line connecting O(Glu80) and N(substrate) atoms (Figure 8). The final step IV refers to the cleavage of the peptide bond accompanied by deprotonation of the hemiacetal complex, thus restoring the carbonyl group of acylenzyme. At this stage the negatively charged Asp170 serves as a general base. The proton transfer to the leaving group is facilitated by the simultaneous proton uptake from Asp84 to Glu80, which in turn is assisted by Ser133. It should be noted that the proton shuttling between Glu80 and Asp84 on the segments III and IV, which appears as a result of the present calculations, may be refined at a higher level computational scheme; however, it should not affect the general conclusions of our modeling.

The above considerations leave room for an assignment of the serine-carboxyl peptidases to a certain class of enzymes, if the mode of substrate activation is taken into account. Generally, the first stage may include nucleophile activation by a general base as in the case of serine proteases at neutral pH[10] or an acid-catalyzed mechanism of the substrate carbonyl group activation by its protonation at lower pH as for carboxyl (aspartic) peptidases.[40] In both cases, the active sites are designed to provide an additional activation of the reaction partner. In serine proteases, an oxyanion hole facilitates the peptide bond hydrolysis by stabilizing TI and, to a certain extent, by activating the substrate carbonyl group by hydrogen bonds.[10] Despite an existing classification of serine-carboxyl peptidases as enzymes of serine-protease type, which is mainly inspired by the structural homology of sedolisins and subtilisins, the results obtained in this work favor the catalytic mechanism similar to that of acid-based hydrolysis of peptides.

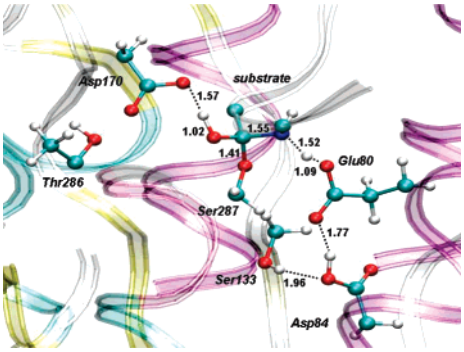

Figure 8. The computed structure of TS2. The distances are shown in Å.

Although tentative proposals on catalytic action of serine-carboxyl peptidases have been formulated by the authors of refs 8 and 11, their assumptions are consistent with an activation stage typical for the serine proteases. When considering the energy changes along a very short part of the reaction path (between the hemiacetal and aldehyde complexes), the authors of ref 11 hypothesize that the role of aspartic acid (Asp170 for sedolisin) is only to stabilize the tetrahedral adduct by donating its proton to the oxyanion actually formed as a result of the general base-activated nucleophilic attack. According to our results (Scheme 1) the protonated aspartate (Asp170 in sedolisin), when standing in a similar position as the oxyanion hole moieties in serine proteases, actively participates in the reaction by donating its proton to the peptide bond of the substrate.

The aspartic acid residue coupled with the glutamate partner (Asp170 and Glu80 in sedolisin) can be considered as a catalytic dyad analogue to the protonated and unprotonated Asp residues in aspartic proteases.[40] The important role of this dyad has been recognized in experimental site-directed mutagenesis studies of different members of the

sedolisin family S53. The pairs of residues Asp360/Glu272 in CLN2,[41,42] Asp164/Glu78 in kumamolisin,[43] and Asp211/Glu86 in aorsin[44] are considered as structural analogues of the Asp170/Glu80 acidic pair in sedolisin. When analyzing kinetic parameters of mutant proteins Asp360/Ala vs Glu272/Ala of human tripeptidyl-peptidase (CLN2), the authors of ref 42 arrived at the conclusion that the catalytic efficiencies were greatly reduced compared to the wild-type enzyme. Similar observations were noticed for kumamolisin,[43] the Asp164/Ala and Glu78/Ala mutants of which did not exhibit proteolytic activity. In the case of aorsin, Asp211/Asn and Glu86/Gln mutations resulted in the loss of catalytic activity by 4 orders of magnitude.[44] Finally, Oyama et al. showed that Asp170/Ala and Asp169/Ala mutants in sedolisin and sedolisin-B, respectively, did not show any autocatalytic processing and proteinase activity.[45] The authors stressed that the Asp170 residue in serine-carboxyl peptidases should be considered as a catalytic residue.[45] Wlodawer et al. reported about an attempt to create a mutant of kumamolisin-As, in which the glutamate residue of the active site was replaced by a histidine in order to mimic the classical catalytic triad of serine proteases.[7] The authors concluded that a normal catalytic triad could not be reconstructed in this case, thus underlining the uniqueness of the glutamate residue in serine-carboxyl peptidases. On the contrary, mutations of the oxyanion hole residues in serine proteases do not show a great impact on the enzyme catalytic activity.[10]

In summary, the computed energy profile for the reaction route from ES to AE for the enzymatic cleavage of a model substrate by sedolisin allows us to formulate conclusions on the reaction mechanism of serine-carboxyl peptidases. As specified in the literature, e.g., in refs 46 and 47, the entropic contributions may slightly change the activation barriers shown in Figure 5 by about 2 kcal/mol without altering the qualitative consequences. According to the results of simulations described in this work, the reaction mechanism of serine-carboxyl peptidases should be viewed as a special case of carboxyl (aspartic) proteases active at acidic pH with the nucleophilic water molecule being replaced by the Ser residue. Despite the structural similarity of sedolisins and subtilisins, the only feature of serine carboxyl peptidases common to serine proteases is the formation of a covalent substrate−enzyme bond at the stage of nucleophilic attack.

Acknowledgment. We thank Prof. A. Wlodawer and Prof. K. Oda for valuable discussions of the project. The substantial contributions of J. Kress and A. Granovsky to the QM/MM extended PC GAMESS version are greatly acknowledged. This work is supported in part by the grants from the Russian Federal Science and Innovation Agency (State contract 02.442.11.7435), from Russian Foundation for Basic Researches (project 04-03-32007), and from the Russian Academy of Sciences (Program 10 of the Division of Chemistry and Material Sciences). We thank the staff and administration of the Advanced Biomedical Computing Center for their support of this project. This project has been funded in part with federal funds from the National Cancer Institute, National Institutes of Health, under Contract No. NO1-CO-12400. The content of this publication does not necessarily reflect the views or policies of the Department of Health and Human Services, nor does mention of trade names, commercial products, or organizations imply endorsement by the U.S. Government.

References

(1) Oda, K.; Sugitani, M.; Fukuhara, K.; Murao, S. *Biochim. Biophys. Acta* **1987**, *923*, 463−469.

(2) Wlodawer, A.; Li, M.; Dauter, Z.; Gustchina, A.; Uchida, K.; Oyama, H.; Dunn, B. M.; Oda, K. *Nature Struct. Biol.* **2001**, *8*, 442−446.

(3) Wlodawer, A.; Li, M.; Gustchina, A.; Oyama H., Dunn, B. M.; Oda, K. *Acta Biochim. Pol.* **2003**, *50*, 81−102.

(4) Wlodawer, A. *Structure* **2004**, *12*, 1117−1119.

(5) Comellas-Bigler, M.; Maskos, K.; Huber, R.; Oyama, H.; Oda, K.; Bode, W. *Structure* **2004**, *12*, 1313−1323.

(6) Wlodawer, A.; Li, M.; Gustchina, A.; Tsuroaka, N.; Ashida, M.; Minakata, H.; Oyama, H.; Oda, K.; Nishino, T.; Nakayama, T. *J. Biol. Chem.* **2004**, *279*, 21500−21510.

(7) Wlodawer, A.; Li, M.; Gustchina, A.; Dauter, Z.; Uchida, K.; Oyama, H.; Goldfarb, N.; Dunn, B. M.; Oda, K. *Biochemistry* **2001**, *40*, 15602−15611.

(8) Wlodawer, A.; Li, M.; Gustchina, A.; Oyama, H.; Oda, K.; Beyer, B. B.; Celmente, J.; Dunn, B. M. *Biochem. Biophys. Res. Comm.* **2004**, *314*, 638−645.

(9) Oda, K.; Nakatani, H.; Dunn, B. M. *Biochem. Biophys. Acta* **1992**, *1120*, 208−214.

(10) Hedstrom, L. *Chem. Rev.* **2002**, *102*, 4501−4523.

(11) Guo, H.; Wlodawer, A.; Guo, H. *J. Am. Chem. Soc.* **2005**, *127*, 15662−15663.

(12) Warshel, A.; Levitt, M. *J. Mol. Biol.* **1976**, *103*, 227−249.

(13) Field, M. J.; Bash, P. A.; Karplus, M. A. *J. Comput. Chem.* **1990**, *11*, 700−733.

(14) Gao, J. L.; Xia, X. F. *Science* **1992**, *258*, 631.

(15) Stanton, R. V.; Hartsough, D. S.; Merz, K. M. *J. Comput.Chem.* **1995**, *16*, 113.

(16) Bakowies, D.; Thiel, W. *J. Phys. Chem.* **1996**, *100*, 10580−10594.

(17) Zhang, Y.; Lee, T.-S.; Yang W. *J. Chem. Phys.* **1999**, *110*, 46.

(18) Murphy, R. B.; Philipp, D. M.; Friesner, R. A. *J. Comput. Chem.* **2000**, *21*, 1442−1457.

(19) Cui, Q.; Elstner, M.; Kaxiras, E.; Frauenheim, T.; Karplus, M. *J. Phys. Chem. B* **2001**, *105*, 569−585.

(20) Alhambra, C.; Corchado, J. C.; Sanchez, M. L.; Gao, J.; Truhlar, D. G. *J. Am. Chem. Soc.* **2000**, *122*, 8197−8203.

(21) Cui, Q.; Karplus, M. *J. Am. Chem. Soc.* **2002**, *124*, 3093.

(22) Cisneros, G. A.; Liu, H.; Zhang, Y.; Yang, W. *J. Am. Chem. Soc.* **2003**, *125*, 10384−10393.

(23) Guallar, V.; Baik, M.-H.; Lippard, S. J.; Friesner, R. A. *Proc. Natl. Acad. Sci. U.S.A.* **2003**, *100*, 6998−7002.

(24) Shurki, A.; Warshel, A. *Adv. Protein. Chem.* **2003**, *66*, 249−379.

(25) Li, G.; Cui, Q. *J. Phys. Chem. B* **2004**, *108*, 3342−3357.

(26) Klähn, M.; Braun-Sand S.; Rosta, E.; Warshel, A. *J. Phys. Chem. B* **2005**, *109*, 15645−15650.

(27) Wong, K. F.; Selzer, T.; Benkovic, S. J.; Hammes-Shiffer, S. *Proc. Natl. Acad. Sci. U.S.A.* **2005**, *102*, 6807−6812.

(28) Shaik, S.; Kumar, D.; de Visser, S. P.; Altun, A.; Thiel, W. *Chem. Rev.* **2005**, *105*, 2279−2328.

(29) Bentzien, J.; Muller, R. P.; Florián, J.; Warshel, A. *J. Phys. Chem. B* **1998**, *102*, 2293.

(30) Torf, M.; Varnai, P.; Richards, W. G. *J. Am. Chem. Soc.* **2002**, *124*, 14780−14788.

(31) Zhang, Y.; Kua, J.; McCammon, J. A. *J. Am. Chem. Soc.* **2002**, *124*, 10572−10577.

(32) Molina, P. A.; Jensen, J. H. *J. Phys. Chem. B* **2003**, *107*, 6226−6233.

(33) Nemukhin, A. V.; Grigorenko, B. L.; Rogov, A. V.; Topol, I. A.; Burt, S. K. *Theor. Chem. Acc.* **2004**, *111*, 36−48.

(34) Morris, G. M.; Goodsell, D. S.; Halliday, R. S.; Huey, R.; Hart, W. E.; Belew, R. K.; Olson, A. J. *J. Comput. Chem.* **1998**, *19*, 1639−1662.

(35) Kal, L.; Skeel, R.; Bhandarkar, M.; Brunner, R.; Gursoy, A.; Krawetz, N.; Phillips, J.; Shinozaki, A.; Varadarajan, K.; Schulten, K. *J. Comput. Phys.* **1999**, *151*, 283−312.

(36) Schmidt, M. W.; Baldridge, K. K.; Boatz, J. A.; Elbert, S. T.; Gordon, M. S.; Jensen, J. H.; Koseki, S.; Matsunaga, N.; Nguyen, K. A.; Su, S. J.; Windus, T. L.; Dupuis, M.; Montgomery, J. A. *J. Comput. Chem.* **1993**, *14*, 1347.

(37) Morris, G. M.; Goodsell, D. S.; Huey, R.; Olson, A. J. *J. Comput.-Aided. Mol. Des.* **1996**, *10*, 293−304.

(38) Goodsell, D. S.; Olson, A. J. *Proteins: Struct., Funct., Genet.* **1990**, *8*, 195−202.

(39) Heteny, C.; Spoel, V. D. *Prot. Sci.* **2002**, *11*, 1729−1737.

(40) Dunn, B. M. *Chem. Rev.* **2002**, *102*, 4431−4458.

(41) Lin, L.; Sohar, I.; Lackland, H.; Lobel, P. *J. Biol. Chem.* **2001**, *276*, 2249−2255.

(42) Walus, M.; Kida, E.; Wisniewski, K. E.; Golabek, A. A. *FEBS Lett.* **2005**, *579*, 1383−1388.

(43) Comellas-Bigler, M.; Fuentes-Prior, P.; Maskos, K.; Huber, R.; Oyama, H.; Uchida, K.; Dunn, B. M.; Oda, K.; Bode, W. *Structure* **2002**, *10*, 865−876.

(44) Lee, B. R.; Furukawa, M.; Yamashita, K.; Kanasugi, Y.; Kawabata, C.; Hirano, K.; Ando, K.; Ichishima, E. *Biochem. J.* **2003**, *371*, 541−548.

(45) Oyama, H.; Abe, S.-I.; Ushiyama, S.; Takahashi, S.; Oda, K. *J. Biol. Chem.* **1999**, *274*, 27815−27822.

(46) Florián, J.; Warshel, A. *J. Phys. Chem. B* **1998**, *102*, 719−734.

(47) Kötting, C.; Gerwert, K. *Chem. Phys.* **2004**, *307*, 227−232.

CT6000686